

*Gambusia* sp., *Puntius* sp. and *Oryzias* sp. Although some of these fish are consumed by local communities, no information is available on the prevalence of infections with heterophyid trematodes in the individuals. The situation, however, demands an in-depth epizootiological study involving a detailed analysis on a seasonal basis, the physico-chemical features of the environment, the prevalence of cercarial infections in the snails and metacercarial infections in the fishes, the role of birds as transmitting agents and the extent of human involvement. Moreover, the snail host in the stream with its broad spectrum of larval trematode infections offers a suitable model for the study of host-parasite-environment interactions.

1. Sewell, S., *Indian J. Med. Res.*, 1922, **10**, 1-327.
2. Sousa, W. P., *J. Exp. Mar. Bio. Ecol.*, 1990, **23**, 273-296.
3. Kuris, A. M., in *Parasite Communities: Patterns and Processes* (eds Esch, G. W., Bush, A. O. and Aho, J. M.), Chapman and Hall, London, 1990, pp. 69-100.
4. Williams, J. A. and Esch, G. W., *J. Parasitol.*, 1991, **17**, 246-253.
5. Fernandez, J. and Esch, G. W., *J. Parasitol.*, 1991, **77**, 528-539.
6. Fernandez, J. and Esch, G. W., *J. Parasitol.*, 1991, **77**, 540-550.

7. Snyder, S. D. and Esch, G. W., *J. Parasitol.*, 1991, **79**, 205-215.
8. Kuris, A. M. and Lafferty, K. D., *Annu. Rev. Ecol. Syst.*, 1994, **25**, 189-217.
9. Mohandas, A., *Folia Parasitol.*, 1974, **21**, 311-317.
10. Mohandas, A., *Ves. Cesk. Spo. Zool.*, 1976, **40**, 196-205.
11. Pande, K. C. and Agarwal, N., *Indian J. Parasitol.*, 1978, **2**, 139-143.
12. Ismail, N. S. and Saliba, E. K., *Riv. Parassit.*, 1985, **46**, 263-271.
13. Ismail, N. S. and Abdel Hafez, S. K., *Helminthologia*, 1987, **24**, 293-301.
14. Miller, H. M. and Northup, F. E., *Bio. Bull.*, 1926, **50**, 490-508.
15. Probert, A. J., *J. Helminth.*, 1966, **40**, 115-130.
16. Erasmus, D. A., *The Biology of Trematodes*, Univ. Press, Belfast, 1972.
17. Africa, C. M., Garcia, E. Y. and Leon, W. De., *J. Philipp. Med. Assoc.*, 1935, **15**, 358-361.
18. Hsu, P. K., *Lignan Sci. J.*, 1951, **23**, 235-256.
19. Martin, W. E., *Trans. Am. Micro. Soc.*, 1959, **78**, 172-181.
20. Pande, B. P. and Shukla, R. P., *Indian J. Anim. Sci.*, 1972, **42**, 971-978.

ACKNOWLEDGEMENT. We thank the UGC, New Delhi for financial assistance.

Received 24 February 1997; accepted 15 March 1997

## On the theory and utility of spectral seismograms

M. Ravi Kumar, D. Sarkar and S. J. Duda\*

National Geophysical Research Institute, Hyderabad 500 007, India  
\*Institute of Geophysics, Bundesstrasse 55, 20146, Hamburg, Germany

A spectral seismogram enables a quick and detailed analysis of an earthquake waveform in terms of the frequency-time distribution of the radiated energy. In this approach, a broad-band signal is first filtered using various bandpass filters to obtain the corresponding bandpass seismograms. Each of these seismograms is then Hilbert transformed, to obtain the corresponding instantaneous amplitudes with respect to time, for each mid-frequency. The resulting amplitudes are then represented using a colour code or a grey scale to obtain a spectral seismogram. We discuss here, the theory of spectral seismograms and as examples, present the spectral seismograms of 3 earthquakes from the Burmese arc region.

AN earthquake source radiates energy over a wide range of frequencies in the form of longitudinal and shear waves. These waves, besides generating various surface waves, get reflected and refracted inside the earth, thereby producing several converted waves. A portion of the seismic energy reaches the surface of the earth, and is recorded by the seismometers. Since the radiated energy spans a wide range of frequencies, it is desirable to

sample an earthquake over as wide a bandwidth as possible, for a better understanding of the earthquake source and the medium through which the waves propagate.

Over the past decade, more than 100 broadband seismometers have been operational worldwide, belonging mostly to networks like IRIS, GEOSCOPE and CDSN. The high quality digital data that is being provided by these broadband instruments now form a fairly extensive data set for modelling the seismic sources and the fine structure of the medium. Spectral analysis of earthquake records has evolved as a powerful tool for analysis of digital data, especially for deciphering the source characteristics.

Spectral analysis using the Fourier transform has been the most powerful and standard means of decomposition of a signal into individual frequency components to obtain the energy spectrum sampled by each component. The energy spectrum thus obtained, however, does not contain information about the time of initiation of these frequencies. An estimate of the variation of the spectrum with time is desirable if one is interested in frequency dependent, time limited signals in a waveform. One way of estimating the time-varying spectrum is to compute the discrete Fourier transform of a sequence of overlapping time intervals that step through a larger time series. The spectrogram<sup>1</sup> utilizes this procedure and has been the most widely used tool for the analysis of time-varying spectra. The concept behind it is simple, yet powerful. In order to analyse what is happening at a particular instant of time, a small portion of the signal

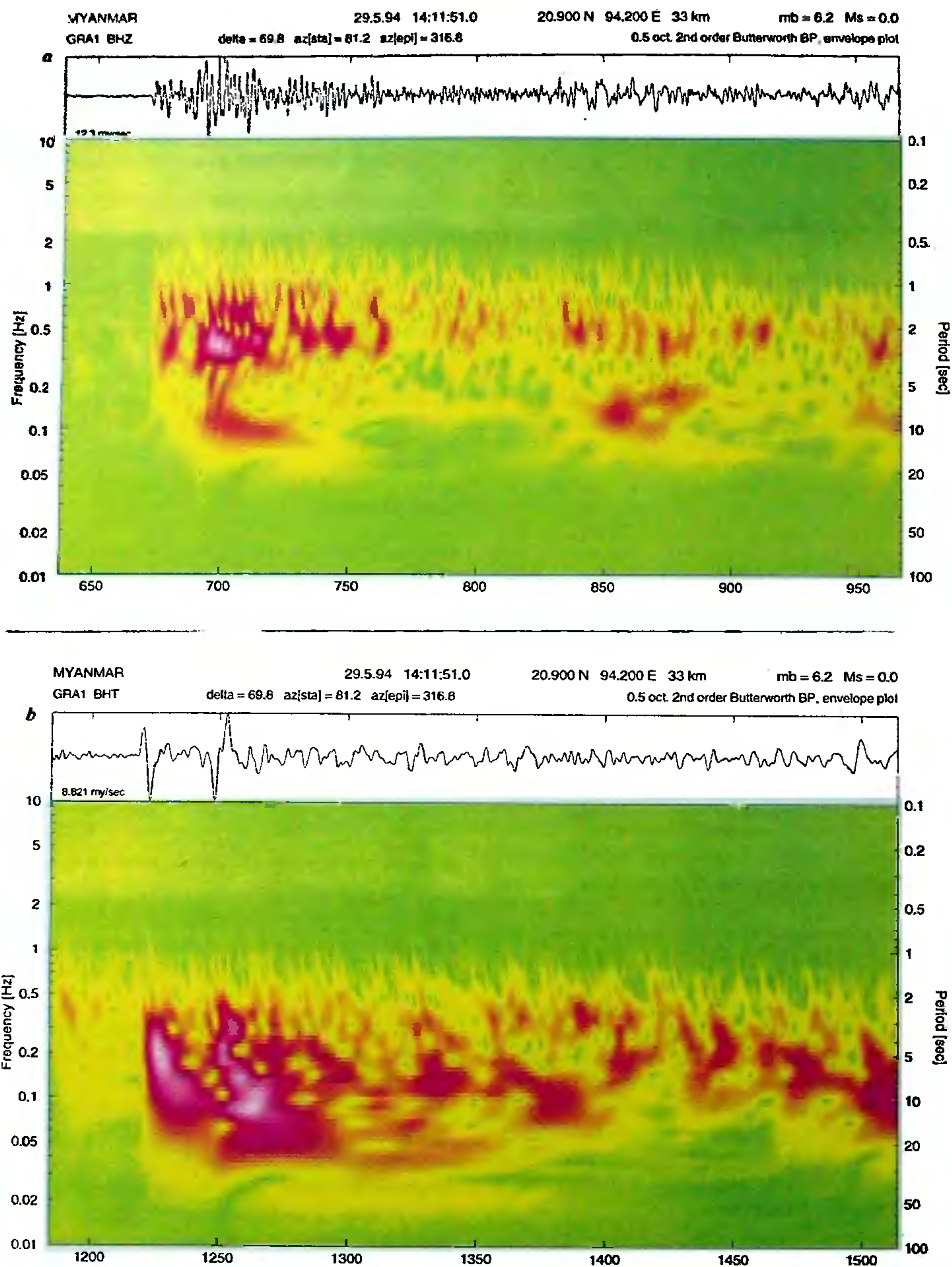


**Figure 1a, b.** Spectral seismograms of the vertical and transverse components of the 29.5.94 Burmese arc earthquake recorded by a Grafenberg station. The corresponding colour code is indicated in Figure 4.

centered around that time is used to calculate its energy spectrum. The same procedure is repeated for each instant of time, using a moving window. However, the

problem arises with the choice of an ideal segment duration for a moving window Fourier transformation. The window may be too short to incorporate long-period

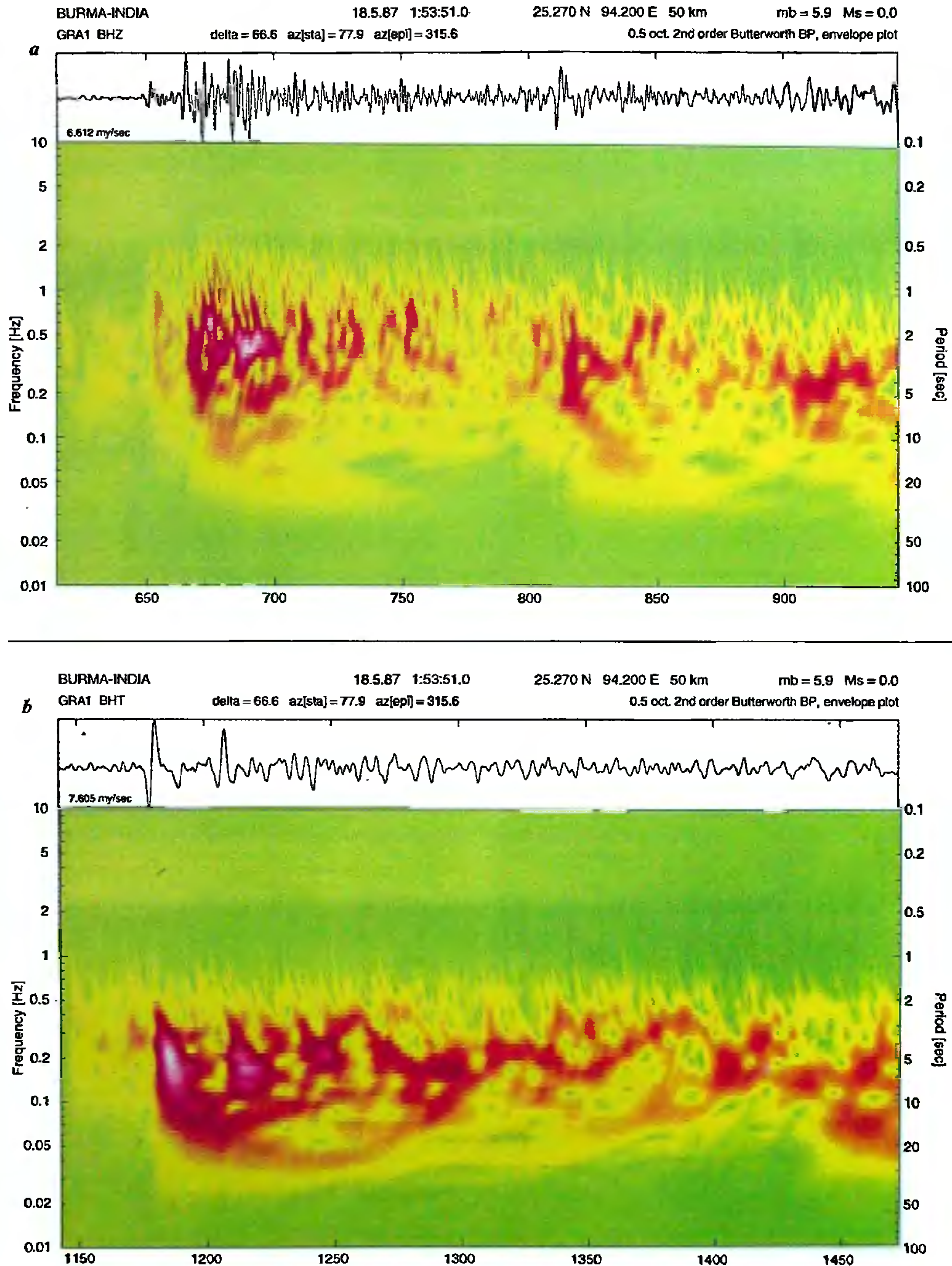


Figure 2 *a, b*. Spectral seismograms of the vertical and transverse components of the 18.5.87 Burmese arc earthquake recorded by a Grafenberg station.

signals adequately or may be too long to resolve changes in the behaviour of short period signals.

For an earthquake signal, the spectral seismogram overcomes this difficulty by resorting to a time-

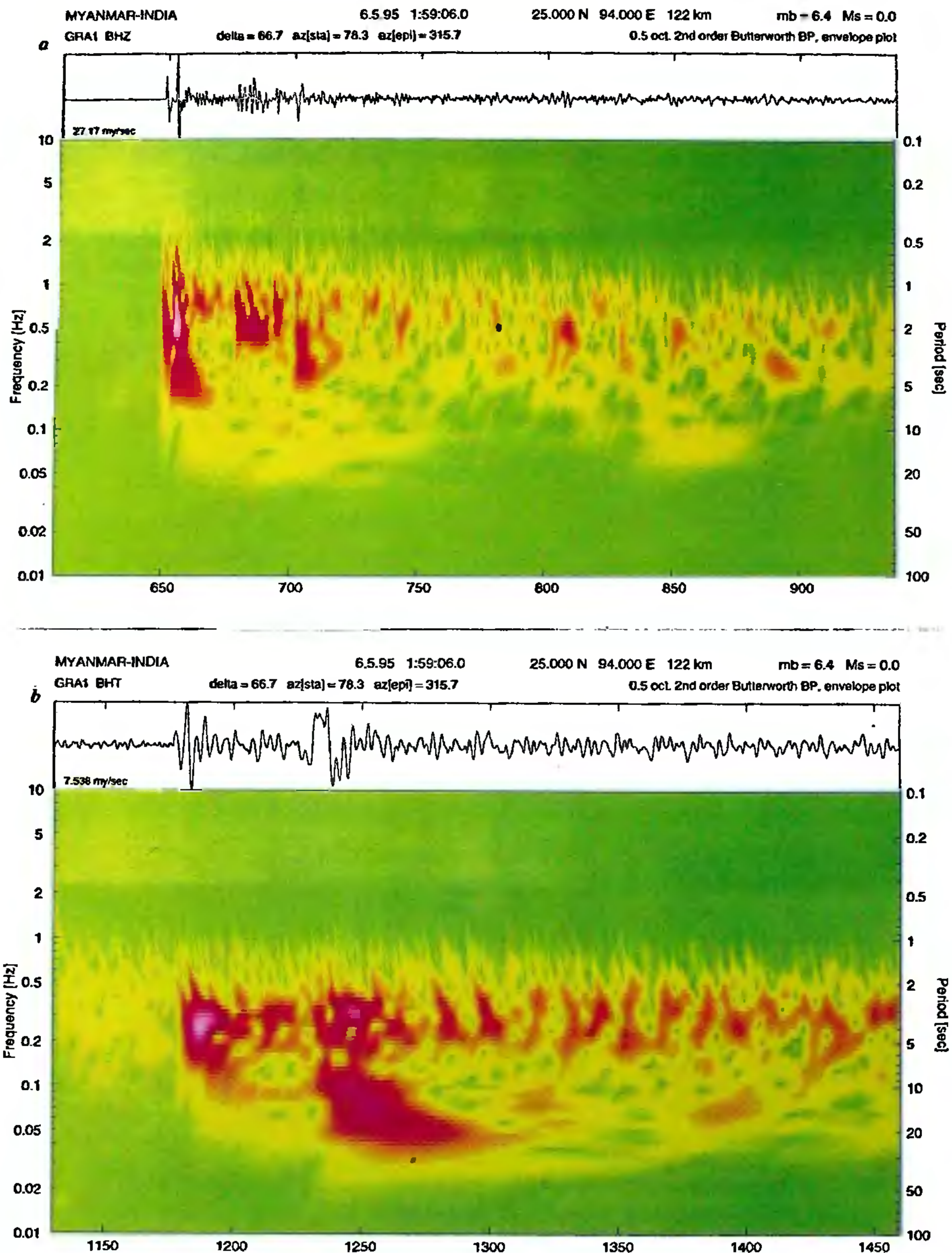


Figure 3a, b. Spectral seismograms of the vertical and transverse components of the intermediate depth 6.5.94 Burmese arc earthquake recorded by a Grafenberg station.

frequency representation of a seismogram, using the instantaneous attributes of a signal, namely, the instantaneous amplitude or envelope and the instantaneous frequency which is the time rate of change of instantaneous phase.

A two dimensional time-frequency representation of a broad-band seismogram is called a spectral seismogram<sup>2,3</sup>. In this approach, a broad-band signal is passed through various narrow band filters centered at varying

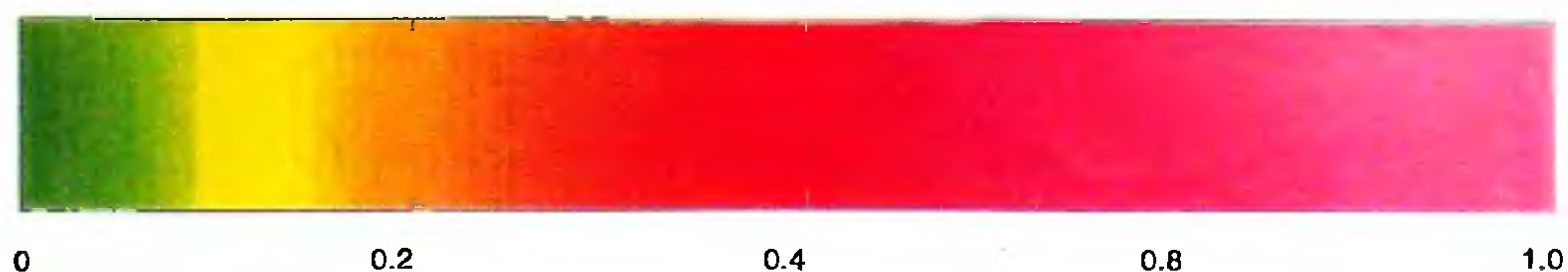


Figure 4. Colour code used to represent amplitudes in the spectral seismograms.

mid-band frequencies, to produce different bandpass seismograms corresponding to the different mid-band frequencies. The instantaneous amplitude or envelope of each of these seismograms is then computed using the concept of an analytic signal<sup>4</sup>.

Given a real time signal  $s(t)$  (a bandpass seismogram in this case), a complex analytic signal  $z(t)$  may be constructed using the relation

$$z(t) = s(t) + iH[s(t)],$$

where  $H$  denotes the Hilbert transform defined as

$$H[s(t)] = \int \frac{s(t-\tau)d\tau}{\pi\tau}.$$

The envelope  $a(t)$  is then the amplitude of the analytic signal given by

$$a(t) = |z(t)| = \sqrt{s^2(t) + H^2[s(t)]}.$$

A plot of the envelopes of all the bandpass seismograms with respect to the corresponding mid-band frequencies represents the frequency-time information of a seismogram. For the convenience of representation, each amplitude is assigned a different colour/intensity, chosen from a pre-defined smoothly varying colour/grey scale.

As examples, we have generated the spectral seismograms of several Indian earthquakes, using the 3-component broad-band data from the GRA1 station of the Grafenberg array in Germany. Though it was ideally desirable to generate spectral seismograms for the entire lengths of the seismograms, depicting the energy distribution of all the seismic phases starting from P up to the surface waves, it was found impractical to present them in a convenient size. As a reasonable compromise, we decided to choose a 5-minute duration of the P and S wave portion of seismograms after the respective theoretical arrival times, corresponding to the IASPEI 91 travel time tables.

Following the procedure described above, each seismogram was band pass filtered using a second order butterworth filter of half octave width. The mid-band frequencies were chosen so as to divide the frequency range spanned by the broad-band seismometer (0.01 Hz to 10 Hz), into 100 equal parts on a logarithmic scale. While the vertical component of the seismogram was utilized to study the frequency-time character of the P

phases, the S phases were studied by computing the radial and transverse components.

In the present study, we have chosen three recent earthquakes which have occurred in the Burmese arc region, where the presence of a subducted Indian lithospheric slab is established down to a depth of about 180 km. The spectral seismograms corresponding to these earthquakes are presented in Figures 1, 2 and 3. In these figures,  $a$  and  $b$  represent the vertical component corresponding to the P wave portion and transverse component corresponding to the S wave portion respectively of the broadband signal. The spectral seismogram of the radial component is not included for convenience of representation. It may be noted that the seismic trace, along with the event information, delta and azimuth with respect to the recording station and the filter parameters used to generate the envelope plot of hundred pass band seismograms are included at the top of each spectral seismogram. The X-axis of the spectral seismogram represents the travel time, Y-axis the frequency/time period. The colour code for the amplitudes is indicated in Figure 4.

It can be observed from Figures 1  $a$  and 2  $a$  that there is a striking similarity in the spectral content of the P wave portions of the seismograms, in the sense that the triplets of the high amplitude around the arrival time of the PcP phase are clearly comparable. It is interesting to note from the CMT solutions that both these earthquakes are of normal type, with a small strike slip component. The shear wave part of the spectral seismograms also appears similar (Figures 1  $b$  and 2  $b$ ). On the other hand, the spectral seismogram of the deeper earthquake (Figures 3  $a$  and  $b$ ) appears markedly different, with the P phases (surprisingly) being richer in high frequencies and the S phases richer in low frequencies, compared to the shallow focus earthquakes. This earthquake has a thrust type of mechanism. It also appears that this earthquake is a double event, as is clear on the P-wave portion of Figure 3  $a$ .

It is interesting to notice concentrations of energies not coinciding with any of the 'expected' phases, corresponding perhaps to reflections from intermediate boundaries, or scattered energy. However, all the expected phases show up prominently on the spectral seismograms, making their identification easier.

Although, at present, the concept of a spectral seismogram is new and its potential yet to be utilized, it is likely to turn out as a powerful tool for routine analysis of seismograms in the near future, since it allows a detailed and quick analysis of the spectral character and time-varying behaviour of an earthquake. This tool can eventually be used to reconstruct the source time history. Also, it may find application in studies of surface wave dispersion, identification of relatively unknown phases and establishing similarities in the spectral character of earthquakes from a similar tectonic setup.

1. Cohen, L., *Proc. IEEE*, 1989, 77, 941–981.
2. Duda, S. J., Grad, M. and Saul, J., IUGG Abstract volume, 1995.
3. Fasthoff, S. and Lúcan, G., personal communication, 1996.
4. Gabor, D., *Proc. IEEE*, 1946, 93, 429–457.

ACKNOWLEDGEMENTS. We thank Dr H. K. Gupta for his guidance and encouragement and J. Saul and S. Fasthoff for computational help and useful discussions. The financial support provided by the DLR, Bonn to M.R.K. and D.S. is gratefully acknowledged.

Received 6 December 1996; accepted 3 March 1997

## An *Aquilapollenites*-associated palynoflora from Mohgaonkalan and its implication for age and stratigraphic correlation of Deccan Intertrappean beds

K. P. N. Kumaran, S. D. Bonde and  
Medha D. Kanitkar

Agharkar Research Institute, G. G. Agarkar Road, Pune 411 004, India

Palynology of the intertrappeans of Mohgaonkalan of Chhindwara District, M.P. has been dealt for the first time. The palynoflorule recovered from the black shale is conspicuous due to the presence of *Aquilapollenites bengalensis*, *Azolla cretacea*, *Gabonisoris vigourouxii*, *Spinizonocolpites echinatus* and *Ariadnaesporites* sp. and is very much comparable with the palynoassemblages of Padwar–Ranipur intertrappean beds of Jabalpur. The palynological data are of significance as they now offer a fine resolution of age of Late Maastrichtian contrary to previous assignment of Early Tertiary on the basis of megafossil evidences. Further, the association of *Aquilapollenites* palynoflora with the dinosaur remains at Mohgaonkalan has been found to be useful for correlation and tagging with the radiometric dates known from various localities of the Deccan basaltic province in Peninsular India. Considering the available palynological data and the dinosaur remains, the intertrappean beds at Mohgaonkalan are also very important for delineating Cretaceous–Tertiary Boundary (KTB) in Deccan Trap Volcanic Episode. In light of new palynological findings, a reappraisal of the Deccan Intertrappean flora and its biostratigraphic implication is needed to critically evaluate the influence of Deccan volcanic activity on the continental terminal Cretaceous biotas.

INTERTRAPPEAN palynofossils are very poorly documented as compared to plant mega fossils due to poor recovery and preservation of them in the trap-associated

sediments. However, in recent years, discovery of more intertrappean horizons bearing carbonaceous facies has proved to be rewarding as the black shales in them are found to be rich in palynological contents<sup>1,2</sup>. While carrying out field work in and around Mohgaonkalan, we came across an unlined well that penetrated through a sequence of black shale-associated intertrappeans and this paper is based on the palynological contents yielded from it. In fact, palynoflora from this area have a significance for a fine resolution of age of the intertrappean beds of Mohgaonkalan in the Chhindwara District of Madhya Pradesh. Moreover, the new palynological data have been found to be useful for stratigraphic correlation of other palynological assemblages and the associated dinosaur-bearing intertrappean beds of the Deccan basalt province of India.

The Mohgaonkalan intertrappean sequence is exposed in an unlined water well situated about 0.5 km west of the village very close to the well-known fossil locality from where a large number of plant megafossils have been documented. The well can be easily located as local people fetch water from it for drinking and irrigation purposes. The intertrappean bed is less than 1 m thick and comprises black shale, greenish shale and light yellowish hard chert. The exact location and details of the intertrappean succession were dealt with recently where in the egg shells of dinosaurian affinities and other faunal elements have been described along with a mention of palynoassemblage<sup>3</sup>. The samples investigated for the present study were collected from material dug out of the water well and in fact, only the black shales have proved to be rich in palynological contents.

The palynological assemblage recovered from the black shales of Mohgaonkalan consists of *Azolla cretacea*, *Aquilapollenites bengalensis*, *Gabonisoris vigourouxii*, *Spinizonocolpites echinatus*, *Triporoletes reticulatus*, *Proxapertites operculatus*, *Tricoplitites* sp., *Cyathidites minor*, *Todsporties* sp., *Ariadnaesporites* sp., *Ephedripites* sp., *Foveosporites* sp. and *Osmundacidites* sp., *Lycopodiumsporites* sp., *Alsophyllidites* sp. The palynofloral assemblage is dominated by *A. cretacea*, *G. vigourouxii* and other laevigate